

Conformational evolution of initially straight flexible and stiff polymers over extended time periods via the scaling law methodology

P. Dimitrakopoulos^{a)}

Department of Chemical Engineering, University of Maryland, College Park, Maryland 20742

(Received 5 June 2003; accepted 18 July 2003)

Knowledge of the conformational evolution of a polymer chain provides invaluable information for all polymer properties. However, the chain evolution is usually determined by monitoring single beads for short times only. In this paper, we numerically determine the configuration evolution over extended time periods by monitoring the eigenvalues of the gyration tensor and applying the scaling law methodology. Results of Brownian dynamics simulations of initially straight chains reveal that after the early free transverse diffusion, flexible polymers exhibit a transverse intermediate-time behavior of $t^{3/4}$, while stiff polymers reveal two intermediate-time behaviors: an early $t^{5/6}$ power law accompanied by a late $t^{3/4}$ evolution. These results are associated with the inherent nonlinearity of the problem. The scaling law methodology we develop in this paper for monitoring the chain configuration should have wide applications in the study of polymer rheology. © 2003 American Institute of Physics. [DOI: 10.1063/1.1607957]

I. INTRODUCTION

The present study considers the conformational relaxation of a single flexible or stiff polymer chain from an initial straight configuration in a viscous solvent. This problem commonly arises when strong flows are turned off in both industrial and biological applications. The problem is also motivated by recent experiments with single DNA molecules relaxing after being fully extended by applied forces as well as by the recent development of microdevices involving stretched tethered biopolymers.¹⁻³ Our interest lies on flexible and stiff polymers, both synthetic such as polyacrylamides, Kevlar, and polyesters as well as biopolymers such as DNA, actin filaments, and microtubules.

Knowledge of the conformational evolution of a polymer chain provides invaluable information for all polymer properties including stress and birefringence. In theoretical studies the configuration evolution is determined by either analytical solutions or numerical calculations. The analytical solutions can predict the chain evolution over extended time periods, but, due to the complexity (and perhaps nonlinearity) of the relevant problems, they are commonly based on unproved assumptions, while their range of validity is not well known. For example, for stiff chains the analytical predictions are commonly based on the assumption of a straight chain; in this case the following question arises: how “straight” should a chain be for a specific analytical prediction to be valid? While this weakness of the analytical studies is valid in any area of science, in the polymer science it is more severe due to the presence of many different length and time scales which give rise to more than one behaviors. For example, in the current problem we show that the polymer chain is practically straight during both short and intermediate times. Should an analytical result based on the straight

chain assumption be valid for short times only, for intermediate times, or for both?

On the other hand, numerical calculations, which can determine the chain evolution accurately (i.e., without the need for any assumption), have been commonly restricted to monitoring single beads over short time periods only. For example, for the problem of the relaxation of an initially straight polymer chain we study in this paper, the chain’s transverse evolution was determined by monitoring the transverse motion of the central bead in the chain⁴ or the motion of individual beads along the chain.⁵ In both studies the monitoring was restricted to short time periods and/or short chains while only the configuration’s dependence on time was found, i.e., not the dependence on the problem parameters (in this case, the polymer length).

This seems to contradict with the computational determination of the stress evolution. In recent numerical studies the polymer stress has been successfully determined over extended time scales by calculating the stress over short time periods only but for different (increasing) polymer lengths, and then applying proper scaling laws. For example, the linear viscoelasticity of semiflexible polymers have been determined over 12 time decades in Refs. 6 and 7, while in Ref. 8 the nonlinear stress relaxation of an initially straight flexible chain was determined over the same time period. Recently, we were able to determine the stress relaxation of an initially extended stiff chain over more than 25 time decades with the utilization of scaling laws.⁹ In principle, the procedure employed for the polymer stress can be extended to the conformational evolution of the polymer chain. Unfortunately, by monitoring the evolution of single beads, one is unable to achieve this goal. The reason is that the single bead motion is affected by local scales only, i.e., the neighbor beads; thus after awhile (usually a few time decades) the single bead relaxation has decayed. The result is that we are unable to verify and understand the full impact of the chain configura-

^{a)}Electronic mail: dimitrak@eng.umd.edu

tion on the polymer properties. This is especially true for the polymer stress, which obviously is affected by the motion of all the length scales of a polymer chain.

Based on the reasoning presented above, to be able to determine the chain evolution over extended time periods, we should monitor a configuration function which involves all length scales, from that of the single bead to the length scale of the entire chain. To achieve this goal, we monitor the evolution of the three eigenvalues of the gyration tensor,

$$\mathbf{R}_G^2 = \frac{1}{N_B} \sum_{i=1}^{N_B} (\mathbf{X}_i - \mathbf{X}_c)(\mathbf{X}_i - \mathbf{X}_c), \quad (1)$$

where \mathbf{X}_i is the position of bead i of the discretized chain, N_B is the number of beads, and $\mathbf{X}_c = \sum_{i=1}^{N_B} \mathbf{X}_i / N_B$ is the center of mass of the chain. Determining the eigenvalues of the gyration tensor is not a new idea. Early studies include the determination of the three eigenvalues of a flexible coil at equilibrium 25 years ago.¹⁰ But most studies restrict their analysis to the static (equilibrium) values of the eigenvalues along with the associated value of the radius of gyration and the end-to-end distance.

In this paper we determine numerically the dynamic evolution of the three eigenvalues of the gyration tensor \mathbf{R}_G^2 . The first (largest) eigenvalue measures the size of the chain along its major axis and can be used to monitor the chain's longitudinal length. (This eigenvalue usually shows a similar behavior to the square of the end-to-end distance and the square of the radius of the gyration R_G^2 .) The other two eigenvalues measure the size of the chain along its two minor axes (i.e., the chain's width), and may be used to study the transverse evolution of the polymer chain. We note that the evolution of the polymer chain is related to the (average) evolution of the chain's monomers (or beads). For example, the transverse evolution of a bead along the polymer contour scales similarly to that for the polymer chain. The numerical procedure is identical to that for the polymer stress, and both properties may be determined simultaneously. In this paper we apply this methodology to a specific problem; namely, to study the configuration relaxation of initially straight flexible and stiff polymer chains. With our methodology, we are able to determine the configuration's dependence on both time t and the problem parameters (for our problem, the polymer length N and chain stiffness E).

We emphasize that an exception in the general trend of the computational studies so far is the recent work of Everaers *et al.*¹¹ who calculated both the longitudinal and transverse fluctuations of semiflexible polymers near equilibrium, and introduced in an organized manner the utilization of scaling laws for the determination of the configuration relaxation over extended time periods. To achieve this goal, the authors recorded the coordinates of one end of the chain as well as both end points as a function of time, and calculated the evolution of the moments and the axis of inertia of the point cloud. (The chain was restricted to relax in the two-dimensional space only). In the present paper, we extend the methodology presented in Ref. 11 by considering other conformational functions (i.e., the eigenvalues of the gyration tensor) appropriate to describe both the length and the width of a polymer chain. We also present a more systematic way

to apply the concept of the scaling laws considering a physical problem with more than one relaxation behaviors.

Thus the purpose of this article is threefold. First, we present configuration functions appropriate to determine both the transverse and longitudinal evolution of the entire polymer chain, from very early times associated with the motion of single beads, to very late times associated with the motion of the entire polymer chain. Second, we further develop the scaling law methodology presented in Ref. 11; the properties of this method are presented with special interest to problems with multiple time behaviors. Third, we apply our methodology to study the conformational relaxation of initially flexible and stiff single polymer chains over extended time periods. Our results are shown to represent the entire relaxation of a long chain over 17 time decades for flexible polymers and over 28 time decades for stiff ones. After a short-time free sideways diffusion, the transverse evolution of flexible chains is shown to exhibit only one intermediate-time behavior described by the power law $t^{3/4}$. On the other hand, stiff polymers reveal two intermediate-time behaviors: an early $t^{5/6}$ evolution accompanied by a late behavior of $t^{3/4}$. The transition at times $\tau_{mid} \sim N^4 E^{-3}$ is also identified. At long times, the chains show only longitudinal relaxation. Our numerical results are accompanied with scaling arguments which help to further understand the polymer relaxation.

We emphasize that the problem we study in this paper is inherently nonlinear, and thus our results should not be confused with those in the linear regime. In this sense, our study complements other studies of nonlinear problems including the inverse problem of the chain straightening by applied forces.^{12,13}

II. MATHEMATICAL FORMULATION

To describe the polymer chain, a discretized version of the wormlike chain model^{15,16} is employed based on a Brownian dynamics method developed in Ref. 4. This method considers a bead-rod model with fixed bond lengths and ignores hydrodynamic interactions among beads as well as excluded-volume effects. The polymer chain is modeled as $N_B = (N + 1)$ identical beads connected by N massless links of fixed length b (which is used as the length unit). The position of bead i is denoted as \mathbf{X}_i , while the link vectors are given by $\mathbf{d}_i = \mathbf{X}_{i+1} - \mathbf{X}_i$. To account for polymer stiffness, a bending energy proportional to the square of the local curvature is added. For a continuous chain $\phi^{bend} = (1/2)\mathcal{E}b \int_0^L (\partial \hat{\mathbf{d}} / \partial s)^2 ds$, where L is the (constant) contour length of the chain and $\hat{\mathbf{d}}$ the local unit tangent. The bending energy \mathcal{E} is related to the persistence length L_p via $\mathcal{E}/k_B T \equiv L_p/b$, where k_B is the Boltzmann constant. The bending energy of the discrete model is given by $\phi^{bend} = \mathcal{E} \sum_{i=1}^{N-1} (1 - \mathbf{d}_i \cdot \mathbf{d}_{i+1} / b^2)$. For a fixed b , the properties of the polymer chain are specified by the number of links N and the dimensionless bending energy $E = \mathcal{E}/k_B T$, or equivalently by the (constant) contour length of the chain L and its persistence length L_p .

Assuming that the bead inertia is negligible, the sum of all forces acting on each bead i must vanish, which leads to the following Langevin equation:

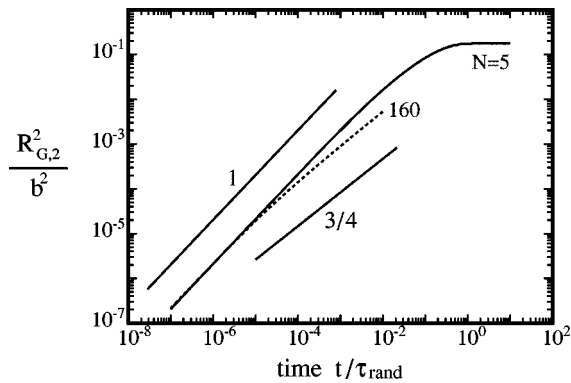


FIG. 1. Transverse evolution of a completely flexible ($E=0$) polymer chain: evolution of the second eigenvalue $R_{G,2}^2$ of the gyration tensor for two representative chain lengths $N=5, 160$.

$$\zeta \frac{d\mathbf{X}_i}{dt} = \mathbf{F}_i^{bend} + \mathbf{F}_i^{rand} + \mathbf{F}_i^{ten} + \mathbf{F}_i^{cor}, \quad (2)$$

where the friction coefficient ζ is assumed to be uniform. The bending force \mathbf{F}_i^{bend} is derived from the chain bending energy, and \mathbf{F}_i^{rand} is the Brownian force due to the constant bombardments of the solvent molecules. The force $\mathbf{F}_i^{ten} = T_i \mathbf{d}_i - T_{i-1} \mathbf{d}_{i-1}$, where T_i is a constraining tension along the direction of each link \mathbf{d}_i , ensures the link inextensibility. Finally, \mathbf{F}_i^{cor} is a corrective potential force added so that the equilibrium probability distribution of the chain configurations is Boltzmann. The resulting system of equations may be solved in $O(N)$ operations.⁴ Ensemble averages are determined employing $10^4 - 10^5$ independent initial configurations. All properties presented in this paper are calculated as ensemble averages of the corresponding instantaneous values. For example, the three eigenvalues of the gyration tensor presented below are calculated as ensemble averages of the instantaneous values of the eigenvalues (and not as the eigenvalues of the ensemble average gyration tensor).

The Brownian forces give rise to a microscopic time scale associated with the diffusive motion of one bead, $\tau_{rand} = \zeta b^2 / k_B T$, which is used as the unit for the times reported in this work if no other unit is used. The numerical method employed in this work has been used to study the linear viscoelasticity of semiflexible polymers⁷ and the non-linear stress relaxation of initially straight flexible polymers,⁸ and will not be discussed further in the present paper.

III. CONFIGURATION RELAXATION OF AN INITIALLY STRAIGHT CHAIN

The transverse evolution of an initially straight flexible ($E=0$) chain is shown in Fig. 1, where we plot the second eigenvalue $R_{G,2}^2$ of the gyration tensor for two representative chain lengths, $N=5$ and 160. The curve for the short chain ($N=5$) reveals the entire transverse relaxation of the polymer chain. At short times the beads follow a free diffusion; the mean-square sideways displacement grows as $R_{G,2}^2 \sim t$. At intermediate times a slower sideways displacement is observed. For the short chain the intermediate-time behavior is limited but it is extended for longer chains. As the figure reveals, for $N=160$ the second eigenvalue $R_{G,2}^2$ shows a

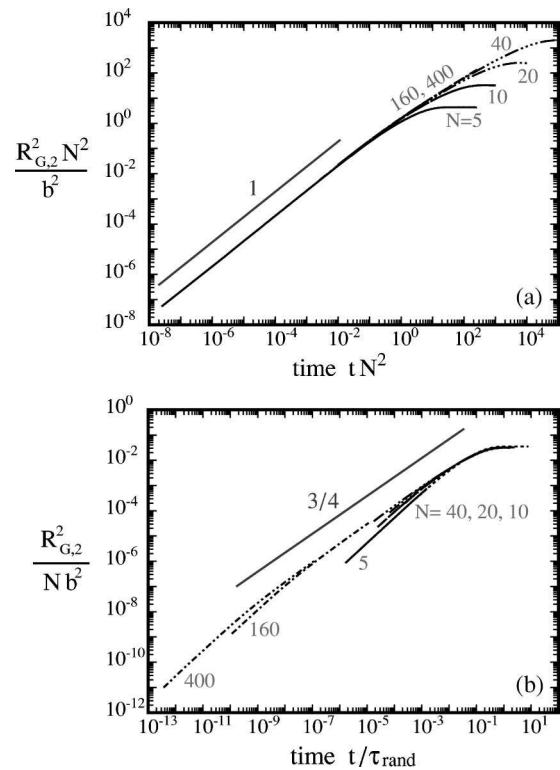


FIG. 2. Scaling law for the evolution of $R_{G,2}^2$ (a) at short times and (b) at intermediate times for a completely flexible chain ($E=0$). Both laws were generated by employing chains with $N=5, 10, 20, 40, 160, 400$.

growth of $t^{3/4}$. Finally, at long times no transverse configuration relaxation is observed; the polymer transverse configuration has come to equilibrium and the evolution of $R_{G,2}^2$ shows a plateau. We note that the evolution of the third eigenvalue $R_{G,3}^2$ is similar and thus the corresponding figure has been omitted. The final value of the two minor eigenvalues is well predicted by the results of Kranbuehl and Verdier,¹⁰ $R_{G,2}^2 = 0.176 R_G^2$ and $R_{G,3}^2 = 0.065 R_G^2$ (i.e., both eigenvalues scale as N at equilibrium).

Immediately after the chain is left to relax from the straight configuration, the transverse component of the tension force on each bead is $F_{\perp}^{ten} \sim T d_{\perp} \sim N^2 t^{1/2}$ since the tensions of the (nearly) straight chain show a $T \sim N^2$ scaling,⁴ while the transverse growth of each bead scales similarly to that of the polymer chain $d_{\perp} \sim R_{\perp} \sim t^{1/2}$. By combining the transverse evolution of each bead with the equation of motion, we conclude that the transverse component of the (effective) Brownian force on each bead scales as $F_{\perp}^{rand} \sim t^{-1/2}$. Thus at short times $t \ll N^{-2}$, $F_{\perp}^{ten} \ll F_{\perp}^{rand}$ and the beads show a free sideways diffusion. During these times the transverse tension force grows faster than the corresponding Brownian force. At the transition times $t \equiv \tau_{ten} \sim N^{-2}$, $F_{\perp}^{ten} \sim F_{\perp}^{rand} \sim N$ and the free diffusion of the beads is arrested.

To show the transverse evolution of the polymer chain at short times and to accurately identify the exact point of the transition, in Fig. 2(a) we plot our results for the full set of polymer lengths (i.e., $N=5, 10, 20, 40, 160, 400$) scaling the time t by its scale at short times N^{-2} and the transverse eigenvalue $R_{G,2}^2$ with its corresponding value N^{-2} . Now the curves for different N fall on each other revealing the chain's

transverse evolution $R_{\perp}^2 \sim t$ over seven times decades. The exact location of the transition is also revealed; as this figure shows, the transition occurs at times $\tau_{ten} \approx 10^{-2} N^{-2}$.

At times $\tau_{ten} \sim N^{-2}$ the link inextensibility is enforced, and thus during intermediate times the transverse motion of each bead affects and is affected by its neighbors. Therefore during these times the transverse evolution of all the chain's segments contribute to the chain relaxation. We note that the chain relaxation is associated with relaxation of tensions (necessary to ensure link inextensibility) from a magnitude of $T = O(N^2)$ at times $t \sim N^{-2}$ to a magnitude of $T = O(1)$ at the end of the intermediate-time behavior at times $t \sim N^2$ for flexible chains.⁴ To reveal the behavior of the chain's transverse evolution at intermediate times $N^{-2} \ll t \ll N^2$, it is still computationally impractical to study a long polymer chain for an extended time period. Clearly a scaling law should be used to match the behavior of chains with different lengths. This idea is employed in Fig. 2(b) where we present the evolution of the second eigenvalue $R_{G,2}^2$ scaled with N (i.e., its scale at long times) for our full set of polymer lengths. Note that the time t has been scaled with the exact value of the time scale for the relaxation of the first normal mode of the Rouse model,

$$\tau_{rouse} = \tau_{rand} \left[12 \sin^2 \left(\frac{\pi}{2(N+1)} \right) \right]^{-1} \quad (3)$$

or $\tau_{rouse} = \tau_{rand} N^2 / (3\pi^2) \sim N^2$ for long chains. As this figure reveals, at intermediate times the mean-square sideways displacement shows a clear growth

$$\frac{R_{G,2}^2}{N} \sim \left(\frac{t}{N^2} \right)^{3/4} \quad \text{or} \quad R_{G,2}^2 \sim N^{-1/2} t^{3/4} \quad (4)$$

over nine time decades.

We emphasize that the $t^{3/4}$ scaling law is associated with the inherent nonlinearity of the current problem. This scaling behavior is further supported by simple scaling analysis. In particular, given the transverse growth of the polymer chain for short and long times, scaling analysis predicts that the observed power-law decay at intermediate times is the simplest power law which can match the transverse growth at short and long times. Observe that at short times $t = O(1/N^2)$ the transverse growth is $R_{G,2}^2 = O(N^{-2})$, while $R_{G,2}^2 = O(N)$ at long times $t = O(N^2)$. Matching these two growths at intermediate times with a single power law t^a gives

$$(R_{G,2}^2)_{short} = N^{-2} (tN^2)^a = (R_{G,2}^2)_{long} = N \left(\frac{t}{N^2} \right)^a \quad (5)$$

which is only valid for $a = 3/4$ and thus at intermediate times $R_{G,2}^2 \sim N^{-1/2} t^{3/4}$ in agreement with our numerical results shown in Fig. 2(b). Our numerical results are also supported by the results of Doyle *et al.*⁵ who numerically calculated the transverse diffusion of individual beads along a single chain with 50 beads and found a growth rate of $t^{3/4}$ over two time decades (as shown in their Fig. 14).

We now turn our attention to stiff polymers and consider the configuration evolution of an initially straight chain with stiffness ratio $E/N = 10$. A similar analysis to that for flexible

chains reveals that at early times the transverse components of the tension and Brownian force on each bead scale similarly to those for flexible chains, i.e., $F_{\perp}^{ten} \sim T d_{\perp} \sim TR_{\perp} \sim N^2 t^{1/2}$ and $F_{\perp}^{rand} \sim t^{-1/2}$. For stiff chains there is an additional force: the transverse bending force $F_{\perp}^{bend} \sim E d_{\perp} \sim ER_{\perp} \sim E t^{1/2}$. (The scaling for this force can be readily derived from the definition of the bending energy ϕ^{bend} .) Thus just after the chain is left free to relax, the effective transverse Brownian force dominates the dynamics and the beads show a free diffusion (i.e., $d_{\perp}^2 \sim R_{\perp}^2 \sim t$) similar to that for the flexible chain. (This conclusion is also supported by our numerical results as we discuss later.) During these times the transverse tension and bending forces grow faster than the corresponding effective Brownian force. The transition from short to intermediate times occurs when one of the two forces, F_{\perp}^{ten} or F_{\perp}^{bend} , balances the transverse Brownian force F_{\perp}^{rand} . Requiring that $F_{\perp}^{ten} \leq F_{\perp}^{rand}$ results in $t \leq N^{-2}$, while the requirement of $F_{\perp}^{bend} \leq F_{\perp}^{rand}$ is valid for $t \leq E^{-1}$. Therefore the first balance reveals the tension time scale $\tau_{ten} \sim N^{-2}$ while the second one reveals the bending time scale $\tau_{bend} \sim E^{-1}$. The latter time scale is the shortest bending mode associated with the transverse fluctuations of two successive links due to the bending energy. (We note that the scaling for τ_{bend} provided above is valid only for large bending energy $E \gg 1$; in a previous work we provided its scaling for any bending energy.⁷)

For stiff chains with $N \leq E \ll N^2$, such as the chains of interest in this paper ($E/N = 10$), we can easily prove that for long enough chains, $\tau_{ten} \ll \tau_{bend}$, and thus the transition from short to intermediate times occurs when the transverse tension force on each bead balances the corresponding Brownian force. On the other hand, a careful examination reveals that for short enough stiff chains the opposite happens, and chains with $N \leq (E/N)$ show $\tau_{bend} \leq \tau_{ten}$. A more accurate description is obtained if we include the numerical coefficient of the two time scales. From Fig. 2(a) we know that $\tau_{ten} \approx 10^{-2} N^{-2}$, while from Fig. 1(c) in Ref. 7 $\tau_{bend} \approx 10^{-3} E^{-1}$. Thus the requirement of $\tau_{bend} \leq \tau_{ten}$ is valid for $N \leq 10(E/N)$. For our problem with $E/N = 10$ we expect that for chains with length $N \leq 100$ the transition from short to intermediate times occurs due to the balance on each bead between the transverse bending and Brownian forces. After this transition at times τ_{bend} , we expect the appearance of an intermediate-time behavior until the end of the transverse relaxation at times $\tau_{\perp} \sim N^4/E$. (The time scale τ_{\perp} represents the longest bending mode associated with the transverse fluctuations of the entire chain due to the bending energy.) For longer chains, the transition from short to the (early) intermediate-time behavior should occur when the growing F_{\perp}^{ten} balances F_{\perp}^{rand} at times τ_{ten} . Afterwards, the relaxation of tensions T (due to the increased transverse evolution) will reduce the tension force F_{\perp}^{ten} . On the other hand, during these times the transverse bending force F_{\perp}^{bend} increases and at some transition times τ_{mid} (to be identified later) will dominate the dynamics. Therefore the evolution of long stiff chains is expected to revert to the evolution of the short stiff chains at late intermediate times (after times τ_{mid} and until the end of all transverse fluctuations at times τ_{\perp}). Thus long enough stiff chains should reveal two different intermediate-

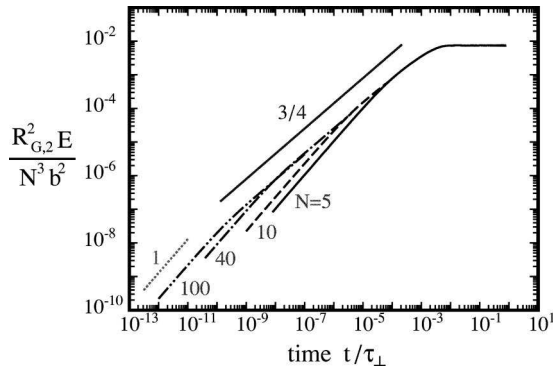


FIG. 3. Scaling law for the evolution of $R_{G,2}^2$ of short stiff polymer chains with $E/N=10$ at (late) intermediate times. The curve was generated by employing chains with $N=5, 10, 40, 100$. Also shown is the free transverse diffusion at short times.

time behaviors. Based on the analysis above, for ultrastiff chains with $E \gg N^2$, $\tau_{bend} \ll \tau_{ten}$ for any polymer length N . (Ultrastiff chains is a stiffness regime we identified in our earlier work.⁷) These chains are expected to follow only one intermediate-time evolution identical to that of short stiff chains.

To prove our reasoning, we plotted our numerical results for the evolution of the second and third eigenvalues at early times for short chains (up to $N=100$), and verified the free transverse diffusion $R_{\perp}^2 \sim t$ at short times $t \ll \tau_{bend}$. The corresponding figure is similar to Fig. 2(a) above (although now we scale the time t with τ_{bend} and $R_{G,2}^2$ with E^{-1}), and thus it has been omitted. To show the relaxation of short chains at intermediate times $\tau_{bend} \ll t \ll \tau_{\perp}$, in Fig. 3 we plot our numerical results for the evolution of the second eigenvalue for chains up to $N=100$, scaling the time t with τ_{\perp} and $R_{G,2}^2$ with N^3/E . We note that the latter value is the scaling of $R_{G,2}^2$ at the final plateau, i.e., when all transverse fluctuations have been decayed, and also its scaling at equilibrium.^{11,14} To understand this scale, we may consider that at equilibrium, $R_{G,2}^2$ should scale as cN^2 where N^2 is the scale for the square length of a stiff chain at equilibrium and c is a coefficient which should be a decreasing function of the stiffness ratio E/N . Our numerical results for different stiffness ratios verify that the coefficient obeys the simple decreasing function $c = (E/N)^{-1}$. Figure 3 reveals that short chains show initially a free sideways diffusion followed by a slower transverse evolution at intermediate times; the latter evolution shown over seven time decades can be described as

$$\frac{R_{G,2}^2}{N^3 E^{-1}} \sim \left(\frac{t}{N^4 E^{-1}} \right)^{3/4} \quad \text{or} \quad R_{G,2}^2 \sim E^{-1/4} t^{3/4}, \quad (6)$$

i.e., it does not depend directly on the polymer length N .

In the case of long stiff chains, by plotting our numerical results for the two minor eigenvalues for long chains ($100 < N \leq 40000$) at early times, we verified the free sideways diffusion $R_{\perp}^2 \sim t$ at short times $t \ll \tau_{ten}$. Note that for these chains the short times extend up to τ_{ten} , and not up to τ_{bend} as for short stiff chains. For this reason the corresponding figure is similar to Fig. 2(a) above with the same scaling for $R_{G,2}^2$ and time t (and thus it has been omitted). Our numerical

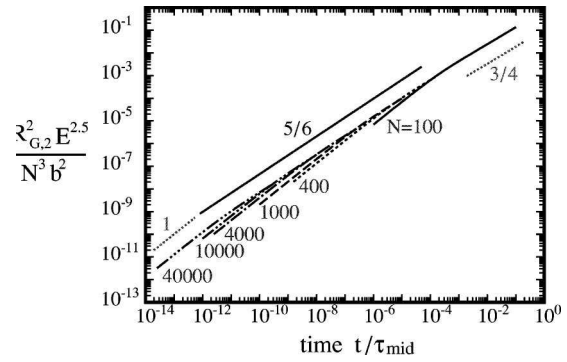


FIG. 4. Scaling law for the evolution of $R_{G,2}^2$ of long stiff polymer chains with $E/N=10$ at early intermediate times. The curve was generated by employing chains with $N=100, 400, 1000, 4000, 10000, 40000$. Also shown are the free transverse diffusion at short times and the $t^{3/4}$ evolution at late intermediate times.

results for these chains also show that after the enforcement of the link inextensibility at times τ_{ten} , the polymer shows a transverse evolution of $t^{5/6}$ valid for all long chains we study in this paper ($100 < N \leq 40000$). From the knowledge of this evolution and the conditions at the transition from short to (early) intermediate times [i.e., $R_{G,2}^2 = O(N^{-2})$ at times $t = O(N^{-2})$], the transition time scale τ_{mid} can be found through scaling arguments. Matching the conditions at the early transition with the scaling law at late intermediate times,

$$(R_{G,2}^2)_{early} \sim N^{-2} \left(\frac{t}{N^{-2}} \right)^{5/6} \sim (R_{G,2}^2)_{late} \sim E^{-1/4} t^{3/4}, \quad (7)$$

we can verify that $t \equiv \tau_{mid} \sim N^4 E^{-3}$.

The transverse evolution of long stiff chains at intermediate times is shown in Fig. 4, where we plot $R_{G,2}^2$ scaled with $N^3 E^{-5/2}$ and time t with $\tau_{mid} \sim N^4 E^{-3}$. We note that $R_{G,2}^2 \sim N^3 E^{-5/2}$ is the value of the minor eigenvalue at the transition times τ_{mid} . [At these times, the chain's transverse evolution at early intermediate times matches that for late intermediate times given by Eq. (6) above.] Figure 4 shows the free sideways diffusion at short times, the power law $t^{3/4}$ evolution at late intermediate times, and also reveals the scaling law at early intermediate times over eight time decades,

$$\frac{R_{G,2}^2}{N^3 E^{-5/2}} \sim \left(\frac{t}{N^4 E^{-3}} \right)^{5/6} \quad \text{or} \quad R_{G,2}^2 \sim N^{-1/3} t^{5/6}. \quad (8)$$

This evolution does not depend directly on the chain stiffness E as we may expect based on our reasoning on the cause for the appearance of this behavior. As happens with the flexible chains, this power-law evolution of the stiff chains is associated with the inherent nonlinearity of the current problem.

While so far we have focused on the transverse evolution of the polymer chain, our methodology may be used to study the relaxation of the longitudinal length of the polymer chain as well. This is shown in Fig. 5 where we plot the evolution of the first eigenvalue $R_{G,1}^2$ of the gyration tensor for an initially straight flexible chain. At short and intermediate times the chain is practically straight; this conclusion is also supported by the small values of the chain's transverse

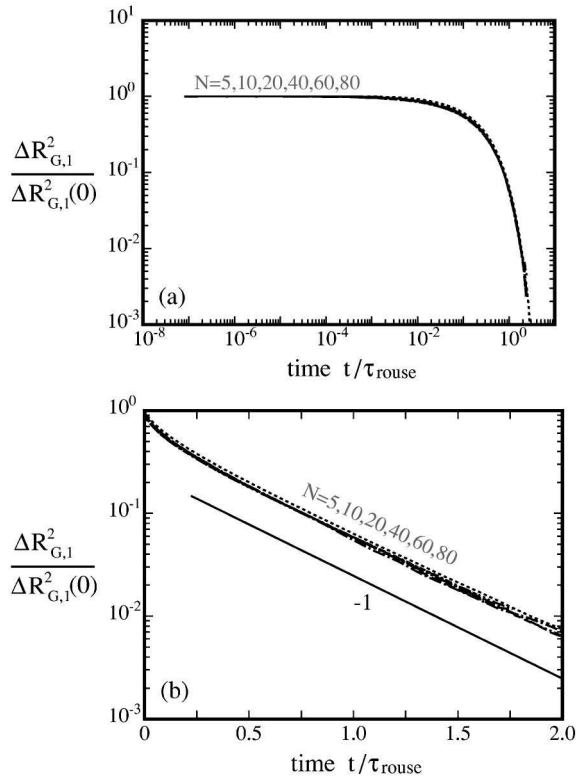


FIG. 5. Longitudinal evolution of the polymer chain. (a) Scaling law for the evolution of the first eigenvalue $R_{G,1}^2$ of the gyration tensor at short and intermediate times for chain length $N=5, 10, 20, 40, 60, 80$. Note that we plot the difference $\Delta R_{G,1}^2 \equiv R_{G,1}^2(t) - (R_{G,1}^2)_{eq}$ [where $(R_{G,1}^2)_{eq}$ is the value of the first eigenvalue at equilibrium] scaled by the value of the difference at time $t=0$, i.e., $\Delta R_{G,1}^2(0) \equiv R_{G,1}^2(0) - (R_{G,1}^2)_{eq}$. (b) Scaling law for the evolution of $R_{G,1}^2$ at long times for the same values of chain length N as in (a).

evolution shown in Figs. 1 and 2 above. At times $t \sim \tau_{rouse}$ the chain shows a sharp decrease in the average polymer length; as revealed in Fig. 5(b), at long times the polymer length shows an exponential decay

$$\Delta R_{G,1}^2(t) \sim N^2 \exp(-2.3t/\tau_{rouse}), \quad (9)$$

where $\Delta R_{G,1}^2(t) \equiv R_{G,1}^2(t) - (R_{G,1}^2)_{eq}$ and $(R_{G,1}^2)_{eq}$ is the value of the first eigenvalue at equilibrium, $(R_{G,1}^2)_{eq} = 0.76(R_G^2)_{eq}$.¹⁰ [Note that the slope of -1 shown in Fig. 5(b) has been multiplied by $\ln 10 \approx 2.3$ in Eq. (9) above.] Our results for stiff chains reveal an exponential decay at long times $t \equiv \tau_{rod} \sim N^3$ but with extended noise due to the fact that a stiff chain at these times is very close to equilibrium. Since at long times the chain shows negligible transverse evolution, we may conclude that the longitudinal relaxation of the polymer chain is the only relaxation mechanism at these times.

As a summary, the transverse relaxation of initially straight flexible polymers shows a free diffusion at short times $t \ll \tau_{ten}$, followed by a power-law evolution of $t^{3/4}$ at intermediate times $\tau_{ten} \ll t \ll \tau_{rouse}$, and then by a plateau at long times $t \geq \tau_{rouse}$. On the other hand, for stiff chains with $N \leq E \ll N^2$, after the short-time free diffusion the transverse evolution follows an early $t^{5/6}$ power law which is accompanied by a $t^{3/4}$ power law during the late intermediate times. At long times, all chains show only longitudinal relaxation.

IV. PROPERTIES OF THE SCALING LAW METHODOLOGY

In this paper we calculate the transverse and longitudinal evolution of both flexible and stiff chains by monitoring the evolution of the eigenvalues of the gyration tensor and applying proper scaling laws. Based on this methodology, we determine the chain's transverse evolution over extended time periods. The two plots provided in Fig. 2 reveal the transverse evolution of a long flexible chain with $N=400$ from several time decades before the tension time scale τ_{ten} up to the end of all fluctuations at times τ_{rouse} . In particular, the conformational evolution is determined from $t/\tau_{rand} = 10^{-7}N^{-2} = 0.625 \times 10^{-12}$ up to $t/\tau_{rand} = 10N^2/(3\pi^2) = 0.54 \times 10^{-5}$, i.e., over nearly 17 time decades. On the other hand, by combining Figs. 3 and 4, the evolution of a long stiff chain with $N=40000$ is revealed from $t/\tau_{rand} = 10^{-14}N^4/E^3 = 0.4 \times 10^{-12}$ up to $t/\tau_{rand} = N^4/E = 0.64 \times 10^{16}$, i.e., over 28 time decades.

We emphasize that the scaling law methodology employed in this paper for the configuration evolution can be used to study other polymer properties as well. We have already mentioned that by employing this methodology we determined the full stress tensor over extended time and length scales.⁷⁻⁹ Thus the properties of the methodology presented below are valid for any polymer property of interest.

(i) The first property of the methodology is that we can extend the scaling laws to any time period we wish. Since short-time scaling laws [such as the one shown in Fig. 2(a) above] represent the earliest time behavior, we can easily extend these laws by adding new curves for any length N and starting the monitoring at earlier times. Scaling laws for intermediate times [such as the ones shown in Figs. 2(b), 3, and 4 above] can be extended by considering longer chains over a proper short time period. Usually five to seven time decades are sufficient for any length N ; the first two to three decades represent the short-time behavior for this length N , while the rest time decades contribute to the scaling law at intermediate times.

We note that to achieve this goal, the different curves should be scaled with the corresponding values at the end of the relevant behavior [as shown in Figs. 2, 3, 4, and 5(a) above]. On the other hand, the long-time behavior (which can only be scaled with the corresponding values at the beginning of the behavior) cannot be extended by utilizing the scaling law methodology [e.g., see the scaling law behavior depicted in Fig. 5(b) above].

(ii) The second property of the methodology is that we should monitor a function which is present during the desired time intervals. The polymer stress is such a function. For the study of the configuration evolution, monitoring the eigenvalues of the gyration tensor always produces useful information, unlike the monitoring of single beads where the useful information is valid for a limited time period only.

(iii) For the best utilization of the scaling law methodology, it is important to realize that the behavior of short chains represents the late behavior of longer chains. This is shown clearly in Figs. 2(b), 3, and 4 above, where the intermediate-time *scaling* behavior based on any (short) chain is extended to earlier times by considering the relaxation of longer

chains. Thus starting from short chains, we can extend the polymer behavior by adding longer and longer chains. This procedure can be repeated indefinitely to any length and stiffness for which the equation of motion, Eq. (2), is valid. Therefore we are able to identify all different time behaviors affecting a specific problem.

(iv) In such a case the following question arises: can we derive two scaling laws from the same figure? The answer is *no* in the general case. To explain this property, we may consider that having two or more scaling laws on the same plot introduces a requirement for the scales of the y and t axis. For example, in the case of two scaling laws showing a power-law behavior of t^a and t^b , respectively, having the laws on the same plot as that of the second law requires that

$$\frac{y \text{ scale for 1st law}}{(t \text{ scale for 1st law})^a} \sim \frac{y \text{ scale for 2nd law}}{(t \text{ scale for 2nd law})^a} \quad (10)$$

which in the general case is not true. (Note that in order to have the two laws on the same plot as that of the first law produces a similar requirement with the only difference that the denominators show a power of b instead of a .) In our problem, expecting to derive the two scaling laws presented in Figs. 3 and 4 above from the same plot as that for the late $t^{3/4}$ law requires that

$$\frac{N^3 E^{-5/2}}{(\tau_{mid})^{5/6}} \sim \frac{N^3 E^{-1}}{(\tau_{\perp})^{5/6}} \quad (11)$$

which does not hold. This property represents a very important point of the scaling law methodology. In several cases by plotting the numerical results from two different laws on the same plot, one may be tricked to derive two laws from the same plot, while only one is valid.

We emphasize that the (negative) property presented above is the reason we present the short- and intermediate-time behaviors of flexible chains into the two plots shown in Fig. 2 above. Similarly we present the early and late intermediate-time behaviors of stiff chains into two different plots (shown in Figs. 3 and 4, respectively). To avoid confusion, we note that each figure shows only one scaling law behavior. For example, Fig. 4 shows the power-law evolution of $t^{5/6}$; the power laws t^1 and $t^{3/4}$ represent single-length evolution and are included in this figure to show the matching with the short-time and late intermediate-time behaviors, respectively.

V. CONCLUSIONS

In this paper we further developed the scaling law methodology¹¹ for calculating polymer properties over extended time periods. In a systematic way, we presented the properties of the method and showed how all the possible time behaviors can be determined for problems with multiple behaviors. We emphasize that the scaling law methodology can be employed to determine various polymer properties simultaneously.

This methodology was employed to study the configuration relaxation of initially straight flexible and stiff chains. To achieve this, we monitored the dynamic evolution of the

eigenvalues of the gyration tensor; these eigenvalues were shown to be appropriate functions to describe both the transverse and longitudinal relaxation of the polymer chain.

The configuration evolution was determined over extended time scales (i.e., over 17 time decades for flexible chains and 28 time decades for stiff ones) as well as polymer lengths. Based on the discussion for flexible chains presented in the Introduction of Ref. 17, identifying our link length b with half the Kuhn length results in $b = 0.065 \mu\text{m}$ for DNA. Thus the maximum length, $N = 400$, we employed in this study for flexible chains corresponds to a DNA molecule with a contour length $L = 26 \mu\text{m}$. This flexibility parameter (contour length over Kuhn length) corresponds to a polystyrene molecule of molecular weight $\approx 140\,000$.¹⁷ In the present study we restricted our results for flexible chains up to polymer lengths $N = 400$ because in this length range all the relevant behaviors were clearly revealed. However, we can easily study much longer chains, at least up to $N = 40\,000$ as our numerical results for stiff chains verify. These lengths correspond to DNA molecules up to 2.6 mm long and to synthetic molecules of polystyrene with molecular weight of $O(10^7)$!

A comparison of the evolution of the second eigenvalue $R_{G,2}^2$ at short and intermediate times presented in Figs. 1 and 2 above with the stress relaxation at the same times (shown in Figs. 1–3 in Ref. 8), reveals that the transition from the short- to the intermediate-time behavior and from the latter to the long-time behavior occurs exactly at the same time for both functions. A similar conclusion can be drawn for the case of stiff polymers which show two different intermediate-time behaviors, as we discuss in a future publication.⁹ These comparisons reveal that the evolution of the eigenvalues is a proper measurement of the configuration evolution for the entire chain and its impact on the stress relaxation.

By employing proper conformational functions (such as the eigenvalues of the gyration tensor) and applying the scaling law methodology, we obtain invaluable information for the chain's evolution over extended time periods which may be used for the understanding of other polymer properties. We emphasize that doing this, we avoid the need to use (approximate) analytical predictions for which the range of validity is generally not well known. Therefore the methodology we developed for monitoring the polymer configuration should have wide applications in the study of polymer rheology.

ACKNOWLEDGMENTS

This work was supported in part by the Minta Martin Research Fund at the University of Maryland. The computations were performed on multiprocessor computers provided by the National Center for Supercomputing Applications in Illinois (Grant No. DMR000003), and by an Academic Equipment Grant from Sun Microsystems, Inc.

¹T. T. Perkins, S. R. Quake, D. E. Smith, and S. Chu, *Science* **264**, 822 (1994).

²T. T. Perkins, D. E. Smith, and S. Chu, In *Flexible Polymer Chains in*

- Elongational Flow*, edited by T. Q. Nguyen and H-H Kausch (Springer, New York, 1999).
- ³G. J. L. Wuite, S. B. Smith, M. Young, D. Keller, and C. Bustamante, *Nature (London)* **404**, 103 (2000).
- ⁴P. S. Grassia and E. J. Hinch, *J. Fluid Mech.* **308**, 255 (1996).
- ⁵P. S. Doyle, E. S. G. Shaqfeh, and A. P. Gast, *J. Fluid Mech.* **334**, 251 (1997).
- ⁶M. Pasquali, V. Shankar, and D. C. Morse, *Phys. Rev. E* **64**, 020802 (2001).
- ⁷P. Dimitrakopoulos, J. F. Brady, and Z.-G. Wang, *Phys. Rev. E* **64**, 050803(R) (2001).
- ⁸P. Dimitrakopoulos (unpublished).
- ⁹P. Dimitrakopoulos and I. D. Dissanayake (unpublished).
- ¹⁰D. E. Kranbuehl and P. H. Verdier, *J. Chem. Phys.* **67**, 361 (1977).
- ¹¹R. Everaers, F. Julicher, A. Ajdari, and A. C. Maggs, *Phys. Rev. Lett.* **82**, 3717 (1999).
- ¹²U. Seifert, W. Wintz, and P. Nelson, *Phys. Rev. Lett.* **77**, 5389 (1996).
- ¹³P. Ranjith and P. B. S. Kumar, *Physica A* **318**, 220 (2003).
- ¹⁴R. Granek, *J. Phys. II* **7**, 1761 (1997).
- ¹⁵M. Doi and S. F. Edwards, *The Theory of Polymer Dynamics* (Clarendon, Oxford, 1986).
- ¹⁶H. Yamakawa, *Helical Wormlike Chains in Polymer Solutions* (Springer, Berlin, 1997).
- ¹⁷R. G. Larson, H. Hu, D. E. Smith, and S. Chu, *J. Rheol.* **43**, 267 (1999).